

# Tract-Based Spatial Statistical Analysis of Diffusion Tensor Imaging in Pediatric Patients with Mitochondrial Disease: Widespread Reduction in Fractional Anisotropy of White Matter Tracts

## ORIGINAL RESEARCH

G.E. Ishak  
A.V. Poliakov  
S.L. Poliachik  
R.P. Saneto  
E.J. Novotny, Jr  
S. McDaniel  
J.G. Ojemann  
D.W.W. Shaw  
S.D. Friedman

**BACKGROUND AND PURPOSE:** Often diagnosed at birth or in early childhood, mitochondrial disease presents with a variety of clinical symptoms, particularly in organs and tissues that require high energetic demand such as brain, heart, liver, and skeletal muscles. In a group of pediatric patients identified as having complex I or I/III deficits on muscle biopsy but with white matter tissue appearing qualitatively normal for age, we hypothesized that quantitative DTI analyses might unmask disturbance in microstructural integrity.

**MATERIALS AND METHODS:** In a retrospective study, DTI and structural MR brain imaging data from 10 pediatric patients with confirmed mitochondrial disease and 10 clinical control subjects were matched for age, sex, scanning parameters, and date of examination. Paired TBSS was performed to evaluate differences in FA, MD, and the separate diffusion direction terms ( $\lambda_r$  and  $\lambda_a$ ).

**RESULTS:** In patients with mitochondrial disease, significant widespread reductions in FA values were shown in white matter tracts. Mean diffusivity values were significantly increased in patients, having a sparser distribution of affected regions compared with FA. Separate diffusion maps showed significant increase in  $\lambda_r$  and no significant changes in  $\lambda_a$ .

**CONCLUSIONS:** Despite qualitatively normal-appearing white matter tissues, patients with complex I or I/III deficiency have widespread microstructural changes measurable with quantitative DTI.

**ABBREVIATIONS:** FA = fractional anisotropy; FSL = FMRIB software library;  $\lambda_a$  = axial diffusivity;  $\lambda_r$  = radial diffusivity; MD = mean diffusivity; MELAS = mitochondrial encephalopathy, lactic acidosis, and stroke-like episodes; MNI = Montreal Neurological Institute; TBSS = tract-based spatial statistics

Mitochondrial diseases<sup>1-3</sup> represent a heterogeneous group of disorders defined by impairment of oxidative phosphorylation. These can manifest in virtually any tissue, often with predominant involvement of the central nervous system. Complex I<sup>4</sup> is the most common electron transport chain abnormality and can result in a range of clinical syndromes including the following: Leber hereditary optic neuropathy, MELAS, myoclonic epilepsy with ragged red fibers, and Leigh syndrome. Typically diagnosis is based on muscle biopsy and enzyme testing, with complex I/III often tested together, with the results supporting complex I or I/III deficits. The most common disorder associated with complex I/III changes is Leigh syndrome, characterized by early childhood onset with a severe progressive course. Bilateral lesions are often seen in the basal ganglia, thalamus, and brain stem with Leigh syndrome.<sup>5</sup> Patients having complex I or I/III deficits

but not clearly defined Leigh syndrome represent a broader phenotype that can include diffuse leukoencephalopathy, pathologically characterized by white matter rarefaction and cystic degeneration.<sup>6</sup>

While diffusion changes are most obviously recognized in tissues in which lesions are present,<sup>7-11</sup> a range of studies have shown the presence of structural changes in tissues that do not appear qualitatively abnormal. DTI has been used to probe tissue features in a variety of conditions, including mild traumatic brain injury, brain tumors,<sup>12</sup> multiple sclerosis, and psychiatric disorders, as examples.<sup>13-15</sup> In mitochondrial disease, a recent study in adults with *m.3243A>G* mutations that did not meet the criteria for MELAS, except for 1 patient, demonstrated FA changes in the occipital lobes, thalami, external and internal capsules, brain stem, cerebellar peduncles, and cerebellar white matter compared with matched control subjects.<sup>16</sup>

Because white matter lesions have been reported in patients with complex I and I/III deficiencies, we hypothesized that quantitative measures of diffusion might be sensitive for detecting subthreshold abnormalities. To test this hypothesis, we identified a group of patients at our center with complex I or I/III deficiencies having qualitatively normal-appearing white matter for age (on T1/FLAIR MR images). Results and a general discussion of how DTI parameters may be more effectively used in routine clinical work are the focus of this report.

Received October 26, 2011; accepted after revision December 24.

From the Departments of Radiology (G.E.I., A.V.P., S.L.P., E.J.N., J.G.O., D.W.W.S., S.D.F.), Neurology (S.L.P., R.P.S., E.J.N., S.M.), and Neurological Surgery (A.V.P., E.J.N., J.G.O.), Seattle Children's Hospital, University of Washington, Seattle, Washington; and Integrative Brain Imaging Center (J.G.O.), University of Washington, Seattle, Washington.

Paper previously presented in part at: Annual Meeting of the American Society of Neuroradiology, June 4-9, 2011; Seattle, Washington.

Please address correspondence to Gisele Ishak, MD, Seattle Children's Hospital, Department of Radiology, 4800 Sandpoint Way, M/S R-5417, Seattle, Washington 98105; e-mail: ishag@u.washington.edu

<http://dx.doi.org/10.3174/ajnr.A3045>

**Patients with complex I or I/III: clinical and biochemical features**

Patient	Age (yr)	ETC Activity		Abnormal Labs	Clinical	MRI Findings
		Complex I	Citrate Synthase			
1	13	15%	96%	None	DD, S, GI-C, H, M, ADHD	Normal
2	13	16.7%	111%	UOA	DD, S, FTT, Micro, A, GI-C	Micro
3	7	25%	100%	UOA, Lac	DD, M, GI-C, H	Normal
4	3	11.7%	140%	UOA	DD, H, M, GI-C	Normal
5	1	4%	94%	CSF	DD, S, FTT, GI-C, M, H	Mild cerebral volume loss
6	8	5%	<5% <sup>a</sup>	None	HA, M, OP	Normal
7	13	0%	100%	None	DD, M, GI, H, OP	Normal
8	4	8%	130%	UOA, Lac-B	H, DD, S, GI, M	Normal
9	2	15%	179%	UOA	DD, M, GI-C, GI, H	Normal
10	5	0%	84%	None	DD, FTT, GI, M	Mild cerebral and cerebellar volume loss

**Note:**—ETC indicates electron chain transfer; UOA, urine organic acids; Lac, lactic acidemia; Lac-B, lactate peak on MRS; CSF, elevated cerebral spinal fluid protein; OP, ophthalmologic abnormality; DD, developmental delay; S, seizures; FTT, failure to thrive; M, muscle weakness/endurance problems; GI, gastrointestinal dysmotility; GI-C, severe constipation; H, hypotonia; Micro, microcephaly; A, autism spectrum disorder; ADHD, attention deficit/hyperactivity disorder; HA = migraine headache.

<sup>a</sup> Complex II was 100% in this patient.

**Materials and Methods**

**Subjects**

Ten patients with mitochondrial disease (6.7 ± 4.9 years, 6 girls/4 boys) were evaluated. Clinical features are shown in the Table. None of our patients had a known mitochondrial syndrome, including specifically MELAS, myoclonic epilepsy with ragged red fibers, Leigh syndrome, or Alpers syndrome, based on clinical and biochemical criteria. The complex I activity was <20% compared with control values and together with the clinical presentation and biochemical findings would meet the criteria of Bernier et al<sup>17</sup> for having mitochondrial disease. These patients could be classified as having multi-systemic mitochondrial disease.

All patients had white matter maturation in the normal range for age, as reviewed by 2 pediatric neuroradiologists. Clinical control subjects all had scan findings read by radiologists as normal, spanning a number of reasons for examinations (6 headache, 1 vertigo, 1 with episode of generalized tonic-clonic seizure, 1 CSF flow query [normal scan findings], 1 ataxia). These patients were matched with those with mitochondrial disease in terms of sex (6 girls/4 boys) and age (within 5.8 ± 6.6 months). The 3 patients younger than 3 years of age were age-matched to controls within 7 weeks of the same age. Patient and control MR imaging data were also matched by the historical date of scanning (within 2.8 ± 4.3 months), to minimize any variability in scanner performance with time, and field strength (3T, *n* = 9; 1.5T, *n* = 1) by using the radiology unified worklist and search tool zVision (<http://www.clariomedical.com>). Retrospective institutional review board approval was obtained by the Seattle Children’s Hospital for inclusion of all participants in this report.

**MR Imaging Data Acquisition**

Imaging was performed on Trio and Allegra magnets (Siemens, Erlangen, Germany) by using phased array coils. Standard clinical imaging included a high-resolution sagittal T1 magnetization-prepared rapid acquisition of gradient echo, axial T2, axial FLAIR, and coronal T2 scans. DTI used a single-shot echo-planar imaging sequence, with imaging parameters varying slightly depending on the scanner used: TE, 92–96 ms; TR, shortest possible; FOV, 230 mm; number of signal intensity-intensity averages, 2–4. The b-values for diffusion-weighting were 0, 1000 s/mm<sup>2</sup>, with 10 gradient-encoding directions. Data were obtained with a matrix size of 128 × 128 and 1.8 × 1.8 mm in-plane resolution. Section thickness was 3.5 mm, with 40 sections covering the entire brain.

**Analysis**

FSL was used for DTI data processing (Version 4.1; FMRIB, Oxford, UK, <http://www.fmrib.ox.ac.uk/fsl>). TBSS (<http://www.fmrib.ox.ac.uk/fsl/tbss/>) was used to perform voxelwise statistical analysis.<sup>18</sup> First, a tensor model fitted to the raw diffusion data created FA images, followed by brain extraction by using the Brain Extraction Tool in FSL.<sup>19</sup> Nonlinear registration was used to align all subjects’ FA data into a common space. Each subject’s aligned data were then projected onto the MNI template image, and voxelwise cross-subject statistics was applied to the resulting data. Maps generated and analyzed were FA, MD, λ<sub>r</sub>, and λ<sub>a</sub>.<sup>20</sup>

Paired *t* tests between patient and control groups were performed with voxelwise analyses and the FSL tool Randomize (<http://www.fmrib.ox.ac.uk/fsl/randomize/>). This method implements permutation-based inference. Multiple comparison correction was performed by using the threshold-free cluster enhancement option, which is recommended for TBSS data.

**Results**

A descriptive comparison of average FA for mitochondrial disease and control subjects is shown in Fig 1. Quantitative comparison for TBSS analyses demonstrated widespread statistically significant differences in FA (*P* < .05, corrected for multiple comparisons), for which values were lower in patients with complex I or I/III compared with control subjects (Fig 2, top row). Specifically, bilateral regions affected included the superior and inferior longitudinal fasciculi; inferior fronto-occipital fasciculus; anterior, superior, and posterior corona radiatae; anterior and posterior thalamic radiations; corpus callosum; external and internal capsules; corticospinal tracts; mesencephalon; pons; medulla oblongata; superior, middle, and inferior cerebellar peduncles; and cerebellar white matter. No regions demonstrated elevated FA in the complex I or I/III group compared with clinical controls.

Group MD analyses are shown in the second row of Fig 2. Consistent increases were observed in patients with complex I or I/III compared with controls; no region demonstrated decreased MD. Maps were generally less attenuated in statistical differences than FA, predominantly in the posterior cerebellum, with most affected regions being the superior and inferior longitudinal fasciculi; inferior fronto-occipital fasciculus; anterior, superior, and posterior corona radiatae; anterior and

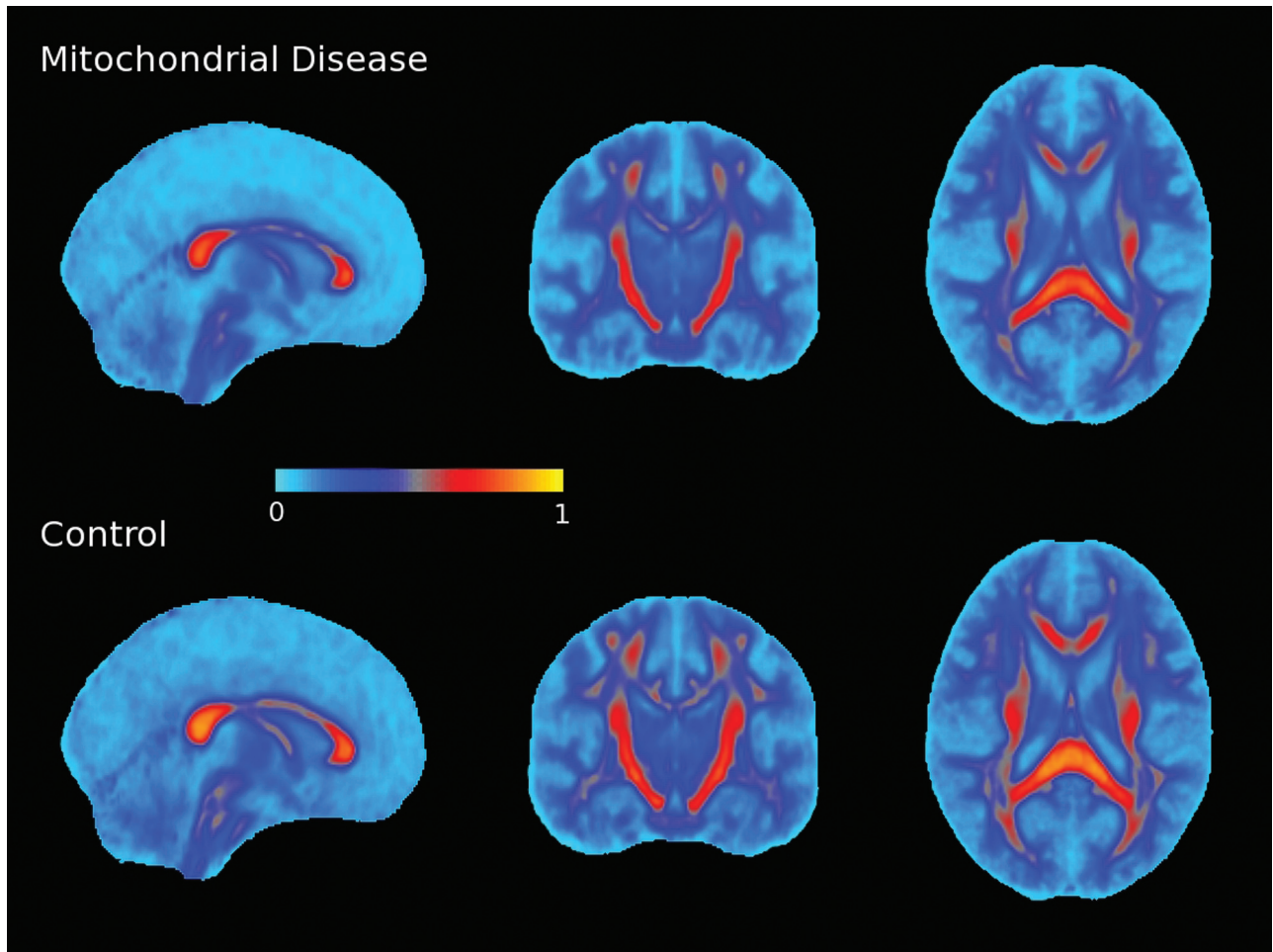


**Fig 1.** Group mean FA value maps for patients with mitochondrial disease and clinical controls. Individual patient FA maps were coregistered to standard space by using the TBSS technique and averaged. The first row shows the group mean FA map for patients with mitochondrial disease complex I or I/III. The second row shows the group mean FA maps for age-matched controls. Even though qualitative analysis of DTI scans (ie, FA, MD, color FA maps, and so forth) showed normal patterns, quantitative analysis revealed widespread reduction in FA values in patients with mitochondrial disease. Values shown were color-coded to highlight subtle differences that may be more difficult to distinguish on gray-scale images.

posterior thalamic radiations; corpus callosum; external and internal capsules; and corticospinal tracts.

Evaluation of radial and axial terms (Fig 2, rows 3 and 4) demonstrated that radial changes are the primary term responsible for the above-noted changes.

### Discussion

White matter abnormalities are seen on imaging with some types of mitochondrial disease, including complex I/III, pathologically characterized by sponginess, deficient myelin formation, myelin loss, abundant presence of lipid-laden macrophages, marked capillary proliferation, prominent gliosis, and eventually also axonal loss. Our purpose was to investigate whether quantitative DTI parameters would detect structural alterations in subjects with complex I/III who did not demonstrate white matter abnormalities on standard MR imaging

Comparing 10 patients with complex I or I/III abnormalities with clinical controls, we demonstrated consistent FA reductions and MD increases in white matter by using TBSS methods. Differences in radial diffusion likely account for most of the explanatory variance, with the caveat that substantial methodologic confounds preclude unambiguous map interpretation.<sup>20</sup> Nonetheless, these consistent changes in FA

support the finding that TBSS methods, compared with paired or population comparison groups, have utility for detecting abnormalities in white matter that can go undetected on qualitative evaluation. Future work pursuing multimodal diffusion and cellular measures such as magnetization transfer<sup>21</sup> or cross-relaxation imaging<sup>22</sup> will be instructive in probing what structural differences in myelin or cell membranes underlie the differences described herein.

Our results overlap somewhat with the previous study by Virtanen et al,<sup>16</sup> which demonstrated widespread FA alterations in a group of patients characterized by *m.3243A>G* mutations, characteristic of MELAS. Most interesting, in that study of adults, group differences were more striking in the posterior and caudal parts of the brain, without MD changes. In our sample, the changes observed were more diffuse and inclusive of MD effects. This may relate to specific complex I or I/III white matter changes or the additional effects of developmental alterations. Further work will be helpful in evaluating the evolution and pattern of changes within other and larger cohorts of patients with mitochondrial disease, in hopes of evaluating concordance in the patterns of observed changes. These results demonstrate the benefit of having quantitative comparisons between age- and sex-matched subjects and,

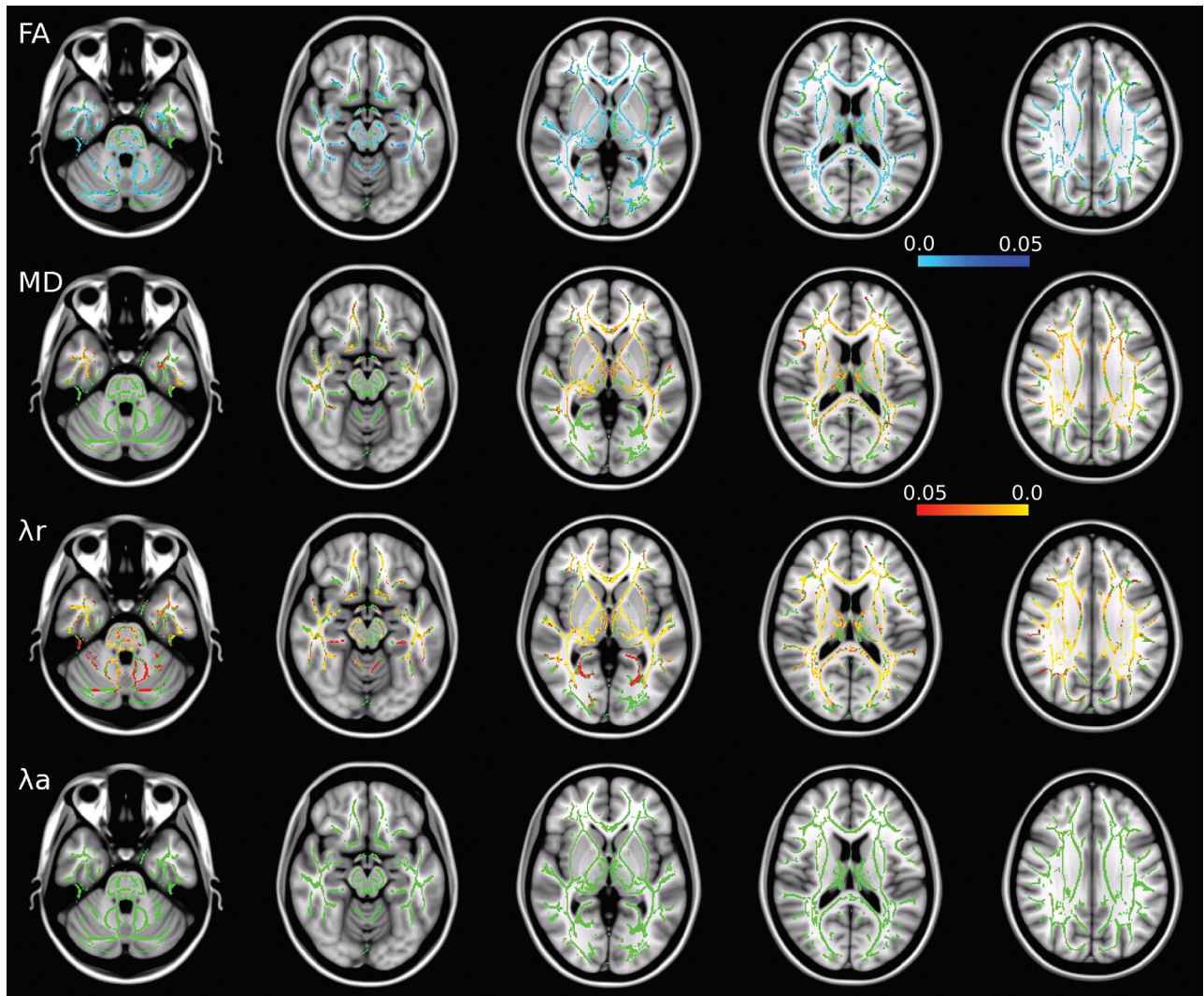


**Fig 2.** Results of TBSS analysis revealed significant differences between the mitochondrial disease and control groups. The figure shows the results of TBSS analysis of DTI parameters (FA, MD,  $\lambda_r$ , and  $\lambda_a$ ) of patients with mitochondrial disease compared with controls (see "Materials and Methods"). Shown in green is the mean FA skeleton, which represents the centers of main white matter tracts. Overlaid on the skeleton are the results of statistical analysis ( $P < .05$ ). Red and yellow represent a significant increase; blue and light blue represent a significant decrease in corresponding DTI parameters. Patients with mitochondrial disease demonstrate widespread decrease in FA and widespread increase in MD and  $\lambda_r$ , while  $\lambda_a$  remains unchanged. Axial sections corresponding to MNI coordinates  $Z = -30, -15, 0, +15, +30$  are shown.

considering the differences not just in group but also in case-to-control comparisons, suggest the potential for clinical utility. Future studies should include comparison with cohorts with leukodystrophies, amino acid disorders, and other biochemical and neurogenetic disorders known to disrupt white matter. Comparison with acquired white matter pathology such as periventricular leukomalacia and traumatic brain injury should also be included. This will be important to determine the specificity and sensitivity of this approach and to define the age-dependent patterns observed in these disorders.

This study has 3 main limitations. The first is the retrospective design and potential selection bias. The second is the small number of patients and controls; however, worth mentioning is the role of nonparametric statistical testing used by FSL. The methods used are more robust for small subject numbers than comparable parametric tests; this consideration is further aided by the paired design of the study.<sup>23</sup> The third limitation is that the controls were obtained from clinically scanned patients and, therefore, potentially differ from healthy popula-

tion controls. Despite being screened for known white matter disorders, the clinical controls may represent a collection of different pathologies, variably expressed. However, this additional variability in the control group is a benefit toward conservatively detecting disease-specific changes. The pairing of samples was necessary to optimize our retrospective experimental design; future studies attempting to more widely implement this method would benefit from collected cohorts arranged in age-specific databases that would allow some evaluation of normalcy on a case-by-case basis. Because these methods may be automated in a research environment, the ability to integrate such measures into the clinical workflow would seem achievable.

### Conclusions

Consistent changes in white matter diffusion were observed in a cohort of patients with mitochondrial disease related to complex I or I/III alterations without overt abnormalities on standard MR imaging. Whether DTI changes represent ana-

tomic regions vulnerable to lesion development with time should be evaluated longitudinally, as well as the potential for these types of methods to provide additional information in understanding the disease processes involved.

### Acknowledgments

The authors acknowledge Weinberger Edvárd for helpful discussions regarding zVision optimization.

Disclosures: Jeffrey Ojemann—RELATED: Grant: Mitochondrial Research grant,\* Comments: Internal (Seattle Children's) grant that funded the work described, Travel/Accommodations/Meeting Expenses Unrelated to Activities Listed: NIH,\* Comments: as part of the grant. Dennis Shaw—UNRELATED: Grants/Grants Pending: NIH,\* Northwest Friends of FacioScapuloHumeral Muscular Dystrophy Research,\* Children's Oncology Group.\* \*Money paid to the institution.

### References

1. DiMauro S, Schon EA. **Mitochondrial disorders in the nervous system.** *Annu Rev Neurosci* 2008;31:91–123
2. Friedman SD, Shaw DW, Ishak G, et al. **The use of neuroimaging in the diagnosis of mitochondrial disease.** *Dev Disabil Res Rev* 2010;16:129–35
3. Saneto RP, Friedman SD, Shaw DW. **Neuroimaging of mitochondrial disease.** *Mitochondrion* 2008;8:396–413
4. Tucker EJ, Compton AG, Calvo SE, et al. **The molecular basis of human complex I deficiency.** *IUBMB Life* 2011;63:669–77
5. Finsterer J. **Leigh and Leigh-like syndrome in children and adults.** *Pediatr Neurol* 2008;39:223–35
6. Zafeiriou DI, Rodenburg RJ, Scheffer H, et al. **MR spectroscopy and serial magnetic resonance imaging in a patient with mitochondrial cystic leukoencephalopathy due to complex I deficiency and NDUFV1 mutations and mild clinical course.** *Neuropediatrics* 2008;39:172–75
7. Brockmann K, Finsterbusch J, Schara U, et al. **Stroke-like pattern in DTI and MRS of childhood mitochondrial leukoencephalopathy.** *Neuroradiology* 2004;46:267–71
8. Ducreux D, Nasser G, Lacroix C, et al. **MR diffusion tensor imaging, fiber tracking, and single-voxel spectroscopy findings in an unusual MELAS case.** *AJNR Am J Neuroradiol* 2005;26:1840–44
9. Duning T, Deppe M, Keller S, et al. **Diffusion tensor imaging in a case of Kearns-Sayre syndrome: striking brainstem involvement as a possible cause of oculomotor symptoms.** *J Neurol Sci* 2009;281:110–12
10. Majoie CB, Akkerman EM, Blank C, et al. **Mitochondrial encephalomyopathy: comparison of conventional MR imaging with diffusion-weighted and diffusion tensor imaging—case report.** *AJNR Am J Neuroradiol* 2002;23:813–16
11. Wieshmann UC, Clark CA, Symms MR, et al. **Reduced anisotropy of water diffusion in structural cerebral abnormalities demonstrated with diffusion tensor imaging.** *Magn Reson Imaging* 1999;17:1269–74
12. Giussani C, Poliakov A, Ferri RT, et al. **DTI fiber tracking to differentiate demyelinating diseases from diffuse brain stem glioma.** *Neuroimage* 2010;52:217–23
13. Wang F, Kalmar JH, He Y, et al. **Functional and structural connectivity between the perigenual anterior cingulate and amygdala in bipolar disorder.** *Biol Psychiatry* 2009;66:516–21
14. Chu Z, Wilde EA, Hunter JV, et al. **Voxel-based analysis of diffusion tensor imaging in mild traumatic brain injury in adolescents.** *AJNR Am J Neuroradiol* 2010;31:340–46
15. Chen Y, An H, Zhu H, et al. **White matter abnormalities revealed by diffusion tensor imaging in non-demented and demented HIV+ patients.** *Neuroimage* 2009;47:1154–62
16. Virtanen SM, Lindroos MM, Majamaa K, et al. **Voxelwise analysis of diffusion tensor imaging and structural MR imaging in patients with the m. 3243A>G mutation in mitochondrial DNA.** *AJNR Am J Neuroradiol* 2011;32:522–26
17. Bernier FP, Boneh A, Dennett X, et al. **Diagnostic criteria for respiratory chain disorders in adults and children.** *Neurology* 2002;59:1406–11
18. Smith SM, Jenkinson M, Johansen-Berg H, et al. **Tract-based spatial statistics: voxelwise analysis of multi-subject diffusion data.** *Neuroimage* 2006;31:1487–505
19. Smith SM. **Fast robust automated brain extraction.** *Hum Brain Mapp* 2002;17:143–55
20. Wheeler-Kingshott CA, Cercignani M. **About “axial” and “radial” diffusivities.** *Magn Reson Med* 2009;61:1255–60
21. Chen JT, Collins DL, Freedman MS, et al. **Local magnetization transfer ratio signal inhomogeneity is related to subsequent change in MTR in lesions and normal-appearing white-matter of multiple sclerosis patients.** *Neuroimage* 2005;25:1272–78
22. Yarnykh VL, Yuan C. **Cross-relaxation imaging reveals detailed anatomy of white matter fiber tracts in the human brain.** *Neuroimage* 2004;23:409–24
23. Nichols TE, Holmes AP. **Nonparametric permutation tests for functional neuroimaging: a primer with examples.** *Hum Brain Mapp* 2002;15:1–25